

Energy Transfer Pathways and Triplet Lifetime Manipulation in a Zinc Porphyrin / F8BT Hybrid Polymer

Jordan Shaikh,[†] David M E Freeman,^{†,§} Hugo Bronstein,^{†,‡} and Tracey M Clarke.^{†,*}

[†] Department of Chemistry, University College London, Christopher Ingold Building, London, WC1H 0AJ, United Kingdom

[§] Department of Chemistry, Imperial College London, Exhibition Road, London, UK SW7 2AZ

[‡] Department of Chemistry, University of Cambridge, Lensfield Road, Cambridge, CB2 1EW, United Kingdom

ABSTRACT: Triplet states are ubiquitous in organic electronics and their properties are increasingly being exploited to enhance device efficiencies. The difficulty in accurately probing triplet states dictates that more fundamental understanding is required of their properties. In this work a hybrid co-polymer of F8BT with 10 % by weight zinc porphyrin was synthesised and a transient absorption spectroscopy study performed. It was observed that a dual energy transfer mechanism was active, whereby the ultimate fate of each photogenerated F8BT singlet exciton depended upon its distance to a porphyrin unit. F8BT excitons generated within the bulk of the F8BT polymer showed typical F8BT photophysics, with the small proportion of F8BT triplets created able to diffuse to and undergo triplet energy transfer to the porphyrin units. In contrast, F8BT singlet excitons formed within their diffusion length to a porphyrin unit displayed singlet energy transfer, followed by ISC to create the lower energy porphyrin triplet. Intriguingly, the F8BT-HAPAPP triplets generated have a lifetime intermediate between the two pristine materials. DFT calculations suggest that this is due to orbital mixing between energetically close benzothiadiazole- and porphyrin-localised molecular orbitals, creating a mixed F8BT/porphyrin triplet state.

Introduction

Triplet states are commonly observed in most optoelectronic devices that rely on conjugated organic small molecules or polymers.¹ Previously, triplets have often been considered a loss mechanism, but the properties of triplets are now being manipulated² in order to achieve beneficial photophysical pathways in conjugated small molecules and polymers, such as photon upconversion,^{3,4} singlet fission,^{5,6} and thermally-activated delayed fluorescence.^{7,8} Despite these recent advances, the properties of conjugated polymer triplets are significantly less well-understood than their singlet counterparts, owing largely to the fact that triplet states are not directly produced upon photoexcitation. As such, key parameters such as triplet absorption cross-sections, quantum yields, population densities, and generation dynamics are much harder to probe accurately. It is therefore vital to establish a greater fundamental understanding of triplet behaviour in such polymers. Due to the lack of strong phosphorescence from conjugated polymers, transient absorption spectroscopy (TAS) offers an excellent methodology to explore triplet behaviour instead. TAS directly monitors the optical absorption of photogenerated transient species such as triplet states, and provides information on the identity, yield and recombination of these transient species. This method is widely-

known and has previously been applied to numerous conjugated polymers.⁹⁻¹⁸ Triplet states display a number of known characteristics in TAS, including excitation density independent first order decay kinetics, a long lifetime on the order of micro – milliseconds, and sensitivity to oxygen (provided the triplet energy is above the singlet oxygen energy level).

In this investigation the well-known conjugated polymer F8BT was co-polymerised with a zinc porphyrin derivative, HAPAPP. Previous work on a different porphyrin/polymer hybrid co-polymer revealed the presence of triplet sensitisation, singlet energy transfer, and a thermal equilibrium between the polymer and porphyrin triplet populations.¹⁹ One motivation behind this work was to establish the generality of these findings, and also to explore the new hybrid polymer's potential for photon upconversion. A zinc porphyrin derivative was used on the basis of its narrow singlet-triplet gap, high triplet yields, and long triplet lifetimes.^{20,21} Furthermore, metal porphyrins have been shown numerous times to act as efficient triplet sensitisers in the solid state.^{22,23} F8BT was chosen as the polymer backbone as it has been shown to undergo TTA in the solid state.²⁴ The triplet energy level of F8BT is found at approximately

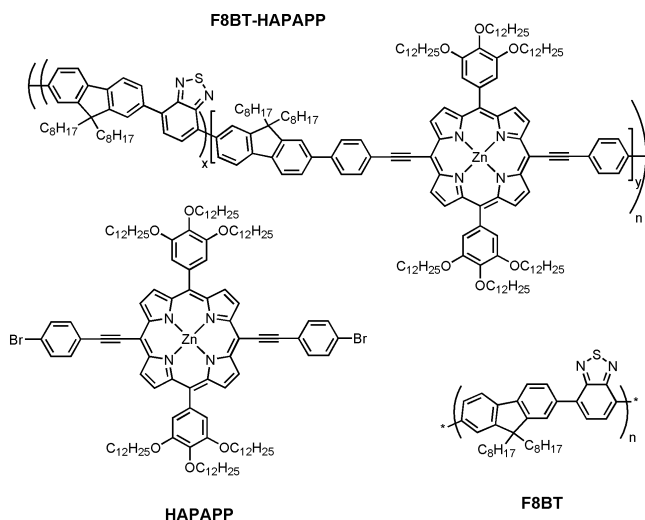


Figure 1. Structures of F8BT, HAPAPP, and F8BT-HAPAPP, where $R = C_{12}H_{25}$.

1.8 eV,²⁵ which is close to the triplet energy of > 1.6 eV found for Zn porphyrins.^{26,27} The resulting hybrid polymer, F8BT-HAPAPP, contains approximately 5 – 10 % by weight of porphyrin. F8BT-HAPAPP, along with the control pristine materials of F8BT and the porphyrin HAPAPP, were investigated using a combination of steady state and time-resolved spectroscopic techniques. It was observed that, irrespective of excitation wavelength, the porphyrin triplet was photogenerated in F8BT-HAPAPP. However, excitation of the F8BT chains of the hybrid polymer enabled two photophysical pathways to generate this triplet: both singlet and triplet energy transfer mechanisms are present simultaneously. Furthermore, it was observed that the F8BT-HAPAPP triplet had a lifetime intermediate between the pristine polymer and porphyrin. Rather than being assigned to a triplet equilibrium, as seen previously,¹⁹ the alteration in lifetime is attributed to a delocalisation of the LUMO over both porphyrin and benzothiadiazole moieties caused by the high level of planarity observed in this porphyrin, creating a triplet with dual F8BT/porphyrin character.

Methods

Synthesis: All synthetic details can be found in the supporting information. F8BT was purchased from Ossila ($M_w = 376,214$) and used without further modification.

Steady state absorbance and fluorescence: Absorbance spectra were recorded with a Perkin Elmer LAMBDA 365 UV/Vis spectrophotometer. Fluorescence spectra were recorded with a Horiba FluoroMax-4 spectrofluorometer, and corrected for instrument response at the exciting wavelength. Steady-state spectra were recorded at room temperature, in chlorobenzene solution (3.4 $\mu\text{g/mL}$).

Nanosecond-microsecond TAS: Microsecond TAS on the solutions was recorded using laser pulses (6 ns, repetition rate 10 Hz) from a Nd:YAG laser (Spectra-Physics, INDI-40-10) and OPO (Spectra-Physics, VersaScan/120/MB) with

pump wavelengths of 460, 518, 640 and 650 nm, using pump intensities of 0.9 – 22 $\mu\text{J cm}^{-2}$. The light output of a quartz tungsten halogen lamp (Bentham, IL1) was used as a probe and signals were recorded with Si and InGaAs photodiodes, housed in a preamplifier and an electronic filter (Costronics Electronics) connected to an oscilloscope and PC. Probe wavelengths were selected with a monochromator (Spectra-Physics, Cornerstone 130 1/8m). Chlorobenzene solutions in a Youngs tap quartz cuvette (Starna Scientific) underwent several freeze-pump-thaw cycles to extract all oxygen, while an oxygen atmosphere was trialled to check for triplet quenching. Concentrations of 34 $\mu\text{g/mL}$, 68 $\mu\text{g/mL}$, and 0.65 mg/mL were used for HAPAPP, F8BT and F8BT-HAPAPP solutions respectively.

Picosecond TAS: Degassed solutions under inert nitrogen atmosphere were excited with pump wavelengths of 518 and 650nm, 2 – 23 $\mu\text{J cm}^{-2}$ pulses, generated by a commercially available optical parametric amplifier TOPAS (Light conversion) pumped by a Solstice Ti:Sapphire regenerative amplifier (Newport Ltd). Changes in the optical density of the films induced by the laser excitation were probed with a second broadband pulse (830 – 1450 nm) generated in a sapphire crystal. A HELIOS (Ultrafast systems) transient absorption spectrometer was used for recording the dynamics of the transient absorption spectra up to 6.5 ns with an average 200 fs instrument response function.

Results

Steady state absorption and photoluminescence.

The structures of poly(9,9-dioctylfluorene-co-benzothiadiazole) (F8BT), HAPAPP (5,15-bis((4-bromophenyl)ethynyl)-10,20-bis(3,4,5-tris(dodecyloxy)phenyl)porphyrin) and F8BT-HAPAPP (poly-2,7-(9,9-dioctylfluorene-alt-4,7-2,1,3-benzothiadiazole)-ran-2,7-(9,9-dioctylfluorene-alt-4',4''-5,15-bis(phenylethynyl)-10,20-bis(3,4,5-tris(dodecyloxy)phenyl)porphyrinato zinc (II))) are shown in **Figure 1**. Synthetic details are reported in the supporting information. The pure F8BT chlorobenzene solution steady state absorption spectrum (**Figure 2**) exhibits two maxima at 322 and 457 nm (3.85 and 2.71 eV). The pure HAPAPP solution absorption spectrum displays an intense Soret band at 450 nm (2.76 eV) and two much weaker Q bands at longer wavelengths, the strongest of which is located at 642 nm (1.93 eV). In the solution of the porphyrin-containing polymer, F8BT-HAPAPP, the absorption spectrum exhibits very little change with respect to the F8BT transitions. However, there is a weak additional peak at 652 nm (1.90 eV), which can be assigned to a red-shifted Q band of the porphyrin incorporated into the polymer backbone. The porphyrin Soret band of F8BT-HAPAPP is obscured by the broader F8BT transition at 457 nm. The very small deviations from the parent F8BT transitions suggest little perturbation of the F8BT backbone upon inclusion of the porphyrin moiety into the polymer. Conversely, the porphyrin seems to possess some degree of electronic perturbation, with its Q-band showing a 0.04 eV redshift relative to the free porphyrin's corresponding Q-band. This

red-shift is consistent with the π -extension of the porphyrin system,^{20,28} due to the greater delocalisation of the HOMO involved in the transition (*vide infra*).

The fluorescence spectra for the three materials are shown in **Figure 3**, all with a pump excitation wavelength of 450 nm. F8BT shows a single emission peak at 544 nm (2.28 eV), while excitation of the free porphyrin, HAPAPP, results in the formation of two emission peaks at 655 and 715 nm (1.89 and 1.73 eV). Excitation of F8BT-HAPAPP results in the formation of a very similar emission profile to that of F8BT. Conversely, excitation of F8BT-HAPAPP at 645 nm reveals solely porphyrin fluorescence, as expected (F8BT does not absorb at this wavelength). As such, it can be concluded that F8BT excitation of F8BT-HAPAPP leads to the bulk of fluorescence occurring from the F8BT before exciton migration to the porphyrin can take place.

Table 1. Quantum yields and lifetimes of F8BT-HAPAPP with selective excitation and the control pristine samples.

Parameter	F8BT excitation		HAPAPP excitation	
	F8BT	F8BT-HAPAPP	HAPAPP	F8BT-HAPAPP
Φ_F	0.85 ^a	0.60 ^a	0.035 ^b	0.086 ^b
τ_{S_1} (ns) ^c	1.9	1.9 and 0.14	1.0	0.9
τ_{T_1} (μ s) ^c	180	460	1000	460

a. Excitation at 400 nm, probe range 475 – 700 nm; b. Excitation at 645 nm, probe range 655 - 800 nm; c. Lifetimes taken from TAS data.

The fluorescence quantum yields for each solution were also measured (**Table 1**). The quantum yield of fluorescence for pristine F8BT was $\phi_f = 0.85$, while that of pristine HAPAPP was 0.035. These numbers reflect the relative efficiencies of the competing relaxation process. HAPAPP, by virtue of its heavy atom, has enhanced spin-orbit coupling and undergoes efficient intersystem crossing to the porphyrin triplet. F8BT, in contrast, has a large S_1 - T_1 energy gap of approximately 0.7 eV and no heavy atom, thus the rate of ISC is low. Furthermore, F8BT has a relatively large S_1 - S_0 energy gap and thus internal conversion is expected to be low as well. The quantum yield of ISC for F8BT, therefore must be a maximum of $\phi_{sc} = 0.15$ (most likely lower). Indeed, a previously estimated value of ϕ_{sc} for F8BT was 0.019.²⁹

The porphyrin-polymer F8BT-HAPAPP produced quite different quantum yield results. Excitation at the porphyrin moiety (645 nm), and encompassing only porphyrin emission from 655 – 800 nm, revealed a fluorescence quantum yield of 0.086, slightly higher than the pristine porphyrin. This may reflect a reduced aggregation of the por-

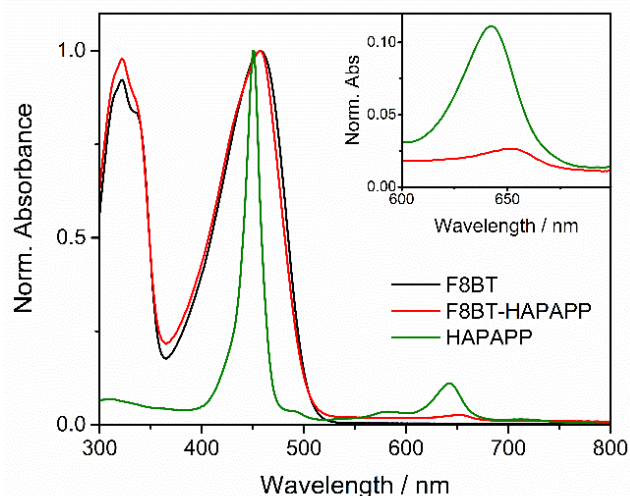


Figure 2. Steady state absorption spectra of F8BT, F8BT-HAPAPP and HAPAPP, in chlorobenzene solution (3.4 μ g/mL). The inset shows the corresponding Q-bands of HAPAPP and F8BT-HAPAPP. Pristine F8BT shows negligible absorption in the red and near infrared.

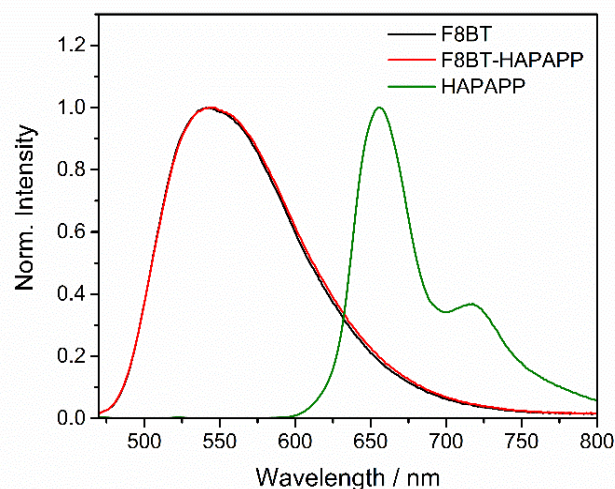


Figure 3. Ground state fluorescence spectra of F8BT, F8BT-HAPAPP and HAPAPP, in chlorobenzene solution (3.4 μ g/mL) with 450 nm excitation.

phyrin in solution, thereby inhibiting self-quenching effects. However, excitation of the F8BT moiety of at 400 nm and probing the F8BT emission at 475 – 700 nm produced a ϕ_f of 0.6, a substantial decrease compared to the pristine F8BT ($\phi_f = 0.85$). This strongly indicates that an additional decay pathway that effectively competes on the timescales of F8BT fluorescence has been introduced by the porphyrin.

Picosecond Transient Absorption Spectroscopy (ps-TAS). Picosecond transient absorption spectroscopy was used to investigate the photophysics of F8BT-HAPAPP,

along with the two controls (F8BT and HAPAPP). A pump excitation wavelength of 518 nm was chosen to selectively excite the pure F8BT and the F8BT moiety of F8BT-HAPAPP. 518 nm was chosen as it gave the same absorbance as the Q-band at 650 nm, and also prevented dual excitation of the narrow porphyrin Soret band at 450 nm. Furthermore, differing concentrations were used such that ground state absorbance at the Q-band was approximately the same for both HAPAPP and F8BT-HAPAPP (Figure S1). The ps-TA spectra are shown in Figure 4.

eV) is found to be generated on ultrafast time scales, exhibiting a short lifetime of 1.0 ± 0.1 ns and thus can be assigned to the porphyrin singlet state, ${}^1\text{HAPAPP}^*$. There is also a rise in signal amplitude from 1000 nm to 900 nm at very early times, suggesting the presence of a second singlet state band in the blank region between the detector limits (< 900 nm). Unlike that of F8BT, the early time spectrum of the pure porphyrin evolves in time to reveal the presence of a much longer-lived species. Features at 540, 750, and 1080 nm (2.30, 1.65, and 1.15 eV) show evidence of growth over time (reaching a maximum amplitude at 3 ns)

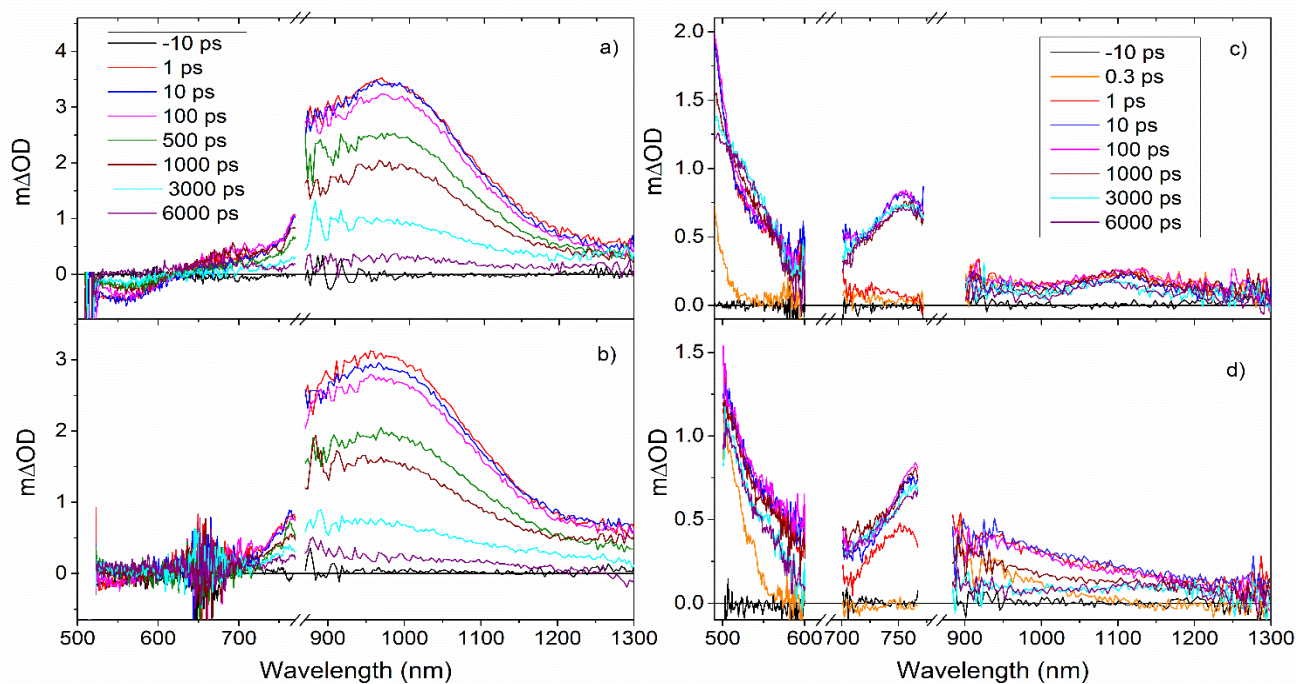


Figure 4. Picosecond transient absorption spectra of a) F8BT excited at 518 nm, b) F8BT-HAPAPP excited at 518 nm, c) F8BT-HAPAPP excited at 650 nm and d) HAPAPP excited at 650 nm. Samples were all in degassed chlorobenzene solution. A concentration of 3.4 mg/mL was used in a) and b). Concentrations of 0.65 mg/mL and 34 $\mu\text{g/mL}$ were used for c) and d) respectively. Spectra were collected with an excitation density of 23 $\mu\text{J cm}^{-2}$ and background corrected. The gap between approximately 800 – 850 nm is the detector change-over region, while the gap centred at 650 nm in (c) and (d) is a result of the laser line.

When excited by 518 nm, the ps-TA spectrum of F8BT (Figure 4a) yields a broad peak at 975 nm (1.27 eV). This peak was fitted to a mono-exponential decay, yielding a lifetime of 1.9 ± 0.1 ns, and is attributed to the F8BT singlet state (${}^1\text{F8BT}^*$). It should be noted that the decay kinetics at 975 nm did not show any laser fluence dependence within the energy regimes employed (2 – 23 $\mu\text{J cm}^{-2}$, see Figure S2). Furthermore, a weak negative signal is present below 600 nm; this was assigned to stimulated emission with a lifetime of 1.8 ± 0.3 ns. The similarity between the lifetimes for the F8BT singlet decay and stimulated emission imply that internal conversion to the ground state is negligible in F8BT, which is reasonable given the large S_1 - S_0 energy gap.

The spectrum created upon excitation of the Q-band of the free porphyrin (a pump wavelength of 650 nm) is shown in Figure 4d. A band peaking below 485 nm (2.56

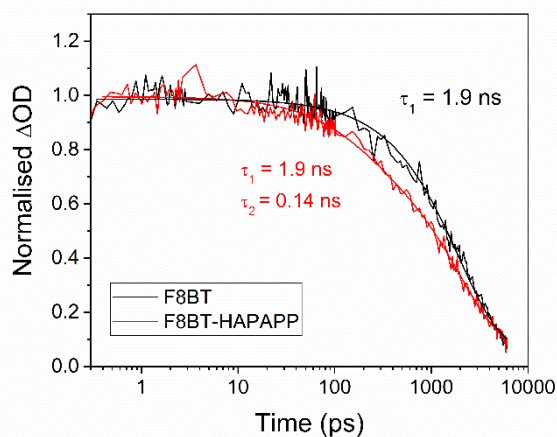


Figure 5. Picosecond transient absorption kinetics of F8BT^a and F8BT-HAPAPP, both excited at 518 nm and probed at 1000 nm with an excitation density of 23 μJ cm⁻², showing the change in kinetics from mono-exponential in the case of F8BT^c to a two-component exponential decay for F8BT-HAPAPP^t.

and exhibit long-lived behaviour: they can therefore be attributed to the porphyrin triplet state, ³HAPAPP*. The observation of these triplet features on the picosecond timescale implies very efficient intersystem crossing (ISC), induced by the heavy Zn atom enhancing spin-orbit coupling. These singlet and triplet assignments are in agreement with previous studies of zinc porphyrins.^{30,31}

Exciting the porphyrin units of F8BT-HAPAPP with a pump wavelength of 650 nm (Figure 4c) yields a spectrum that has distinct similarities to that of the free porphyrin. The strong transition below 485 nm (previously assigned to the porphyrin singlet) is still observed, largely due to an apparent red-shift of this feature, despite absorption of the probe beam in this region by the F8BT ground state. The second porphyrin singlet state band at longer wavelengths is also more noticeable in the case of F8BT-HAPAPP, with the rise in signal amplitude beginning at 1100 nm. This band is found to decay quickly on early timescales, and fitting of the early component at 1000 nm yields a lifetime of 0.9 ± 0.1 ns. This lifetime is close to that found for the free porphyrin singlet, therefore supporting the assignment of this band to the porphyrin singlet state. The redshift of both these porphyrin singlet state bands from HAPAPP to F8BT-HAPAPP is consistent with the redshift observed in the Q bands in the steady state absorption (Figure 2). Similarly, the main F8BT-HAPAPP porphyrin triplet peak, found previously at 750 nm for the pristine porphyrin, is redshifted such that the peak is beyond the detector limit. The less intense triplet transition previously found at 1080 nm in the free porphyrin picosecond spectrum can now only be observed from 3 ns onwards, once the porphyrin singlet signal has decayed sufficiently.

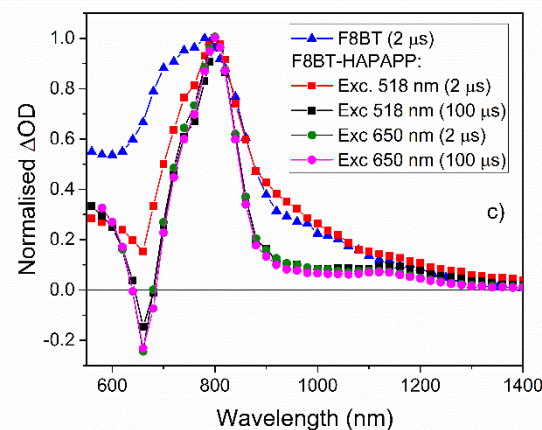
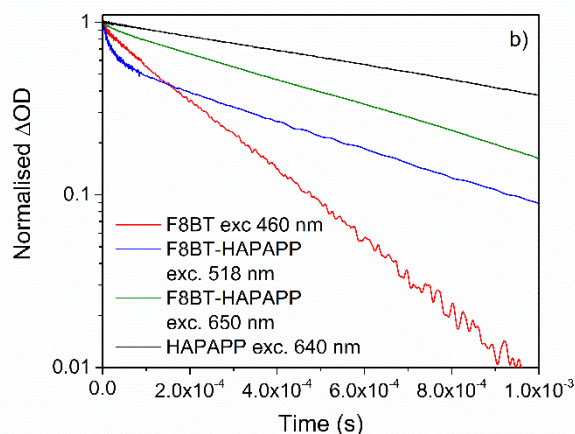
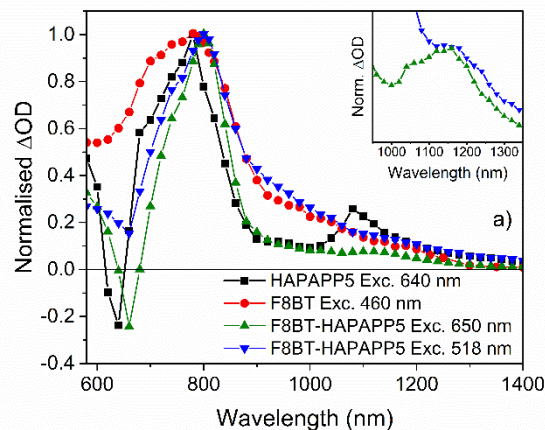


Figure 6. a) Microsecond transient absorption spectra taken at 1 μs in solution. Spectra are normalised to their respective peak maxima. The inset enhances the spectral area of 950-1350 nm for F8BT-HAPAPP, illustrating the characteristic porphyrin peak at both excitation wavelengths. b) Microsecond transient absorption decay kinetics. Kinetics are normalised to the decay value at 1 μs. c) Normalised TA spectra of F8BT-HAPAPP using 518 and 650 nm excitation at 2 μs and 100 μs, compared to F8BT, showing the spectral evolution from an F8BT triplet to a HAPAPP triplet with 518 nm excitation. Samples were in degassed chlorobenzene. Concentrations were 68 μg / mL, 0.65 mg / mL and 34 μg / mL for F8BT, F8BT-HAPAPP and HAPAPP respectively.

Exciting the F8BT backbone of F8BT-HAPAPP with 518 nm (Figure 4b) creates a near identical transient absorption profile to that of the pristine F8BT control. However, the peak at 975 nm, previously assigned to the F8BT singlet, no longer decays monoexponentially. Instead, the ki-

netics of F8BT-HAPAPP can be fitted to a double monoexponential, one component with the original lifetime of 1.9 ns (~ 80% contribution) and the other with a much faster lifetime of 140 ± 20 ps (~ 20 % contribution).

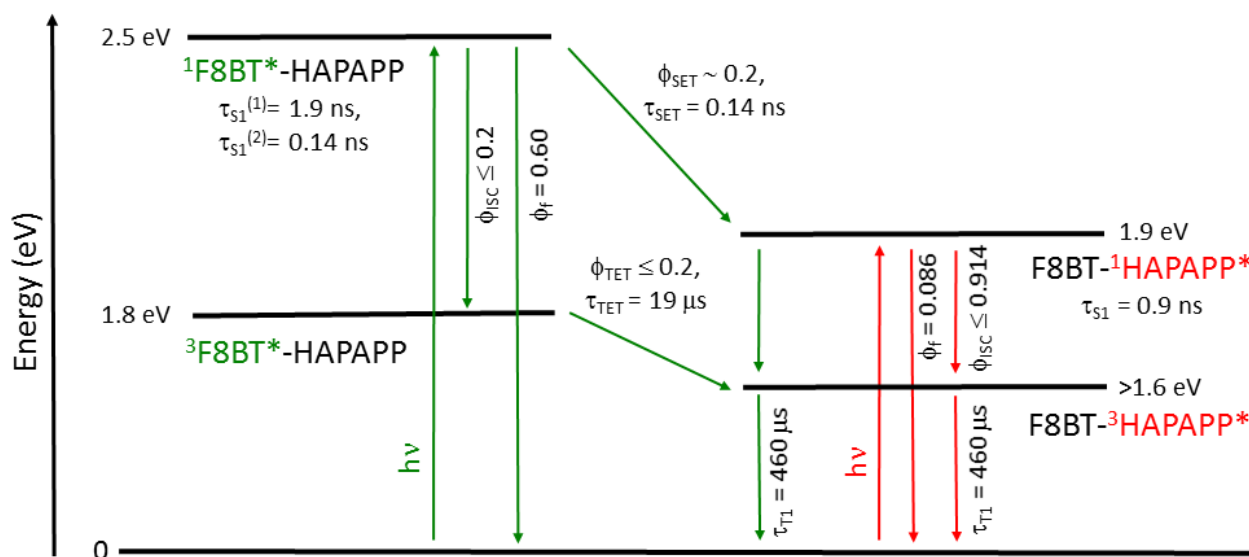


Figure 7. State diagram for the proposed photophysical mechanism in F8BT-HAPAPP solution (not to scale). Since the S₁-T₁ gap of conjugated polymers is usually invariant at (approximately) 0.7 eV, the F8BT T₁ energy is approximately 1.8 eV, since analysis of the steady state absorbance and emission spectrum suggest the S₁ state to be at 2.5 eV in solution. Internal conversion is not shown. The green colour denotes excitation of the F8BT while the red colour denotes porphyrin excitation.

The compared kinetics are shown in **Figure 5**. Interestingly, the stimulated emission below 600 nm is substantially weaker for F8BT-HAPAPP. The fast component observed in the F8BT singlet decay can be assigned to singlet energy transfer to the lower energy porphyrin singlet state. Since porphyrin units comprise less than 10% of the polymer chain, however, most F8BT excitons are generated beyond the exciton diffusion length to a porphyrin unit. These F8BT singlets, therefore, undergo the standard F8BT relaxation and fluorescence processes and exhibit the original ¹F8BT* lifetime. The expected porphyrin singlet feature below 1000 nm is likely obscured by the much more intense F8BT band (which occurs at the same place). The other porphyrin singlet band occurs below 600 nm, but this coincides with the F8BT stimulated emission. This may therefore be one of the reasons for the weaker stimulated emission peak for F8BT-HAPAPP: it is being partially cancelled by the emerging positive porphyrin singlet peak. The lack of observation of ¹HAPAPP* peaks expected from singlet energy transfer is exacerbated by the low porphyrin singlet generation rate of approximately 20 %. As such, the transient spectrum is dominated by the F8BT behaviour. However, the presence of an additional singlet energy transfer pathway is consistent with the decrease in quantum yield of F8BT upon inclusion of the porphyrin to the

F8BT chain. This singlet energy transfer hypothesis was then tested using microsecond TAS, in order to assess the long-lived transient species that form in each case.

Microsecond Transient Absorption Spectroscopy (μs-TAS). The μs-TA spectra measured at 1 μs for the three materials are displayed in **Figure 6a** and the corresponding kinetics in **Figure 6b**. Once again differing concentrations are used in order to excite similar ground state absorbances at each excitation wavelength (Figure S1). When the neat F8BT solution is excited at 460 nm a broad peak is measured at 780 nm (1.59 eV). The F8BT transient spectrum is of similar shape to previous photoinduced absorption studies of F8BT, which was attributed to a triplet transition.³² The peak at 780 nm was found to decay monoexponentially with a lifetime of 180 ± 40 μs, and the signal is completely quenched when the solution is degassed with pure O₂. These features are highly indicative of the F8BT triplet state. Note that this lifetime was acquired at room temperature and it is well-known that the F8BT triplet lifetime is strongly temperature-dependent.³³ No spectral response is observed from F8BT with an excitation wavelength of 650 nm (**Figure S3**).

Exciting the free porphyrin, HAPAPP, with a pump wavelength of 640 nm yields two distinct peaks at 780 and 1080 nm (1.59 and 1.15 eV), both of which decay with the same lifetime of 1.0 ± 0.1 ms. These peaks are quenched by the presence of oxygen. The long lifetime, oxygen quenching, and strong similarity to the ps-TA data at longer times indicate that these peaks can be assigned to the porphyrin triplet state. It should be noted that the main triplet transition in the case of both F8BT and HAPAPP occurs at an identical wavelength of 780 nm. There are three primary differences between the two triplets. The 780 nm band of the porphyrin triplet is much narrower and the lifetime of the porphyrin triplet is almost five times longer. Finally, the porphyrin has an additional triplet peak at 1080 nm, which is entirely absent in the $^3\text{F8BT}^*$ spectrum.

Selective excitation of the porphyrin Q-band in F8BT-HAPAPP with a pump wavelength of 650 nm yields a very similar oxygen-sensitive spectrum to the pristine porphyrin, as expected. As observed in both the steady state and ps-TA spectra, red shifts of the peaks are observed relative to the pristine porphyrin. The F8BT-HAPAPP porphyrin triplet decay kinetics could be fitted to a single monoexponential with a lifetime of 460 ± 40 μs . Intriguingly, the primary decay component's lifetime of 460 μs matches neither the F8BT nor the pristine porphyrin triplet decay. Instead, the F8BT-HAPAPP porphyrin decay lifetime is intermediate between these two.

Selectively exciting the F8BT moiety in F8BT-HAPAPP with 518 nm results in quite different behaviour. Once again, the spectrum can be assigned to a triplet, owing primarily to the oxygen quenching observed. At times longer than 100 μs , the spectrum bears a strong resemblance to the HAPAPP triplet due to the identification of the second porphyrin triplet transition at 1150 nm. However, the decay dynamics of the main 800 nm peak are not purely monoexponential. Two mono-exponential components are fitted possessing lifetimes of 19 ± 3 μs and 460 ± 20 μs , where the fast phase contributes approximately 40 % to the overall decay. The fast component is unlikely to be due to triplet-triplet annihilation, as its magnitude relative to the slow phase does not change with excitation density. The slow phase lifetime of 460 μs is identical to that of the F8BT-HAPAPP porphyrin triplet measured with 650 nm excitation. As such, selective excitation of the F8BT results in porphyrin triplet formation on long timescales, not the F8BT triplet. Once the singlet energy transfer observed in the picosecond TAS takes place, the porphyrin singlet undergoes ISC to generate the porphyrin triplet observed on the microsecond timescales.

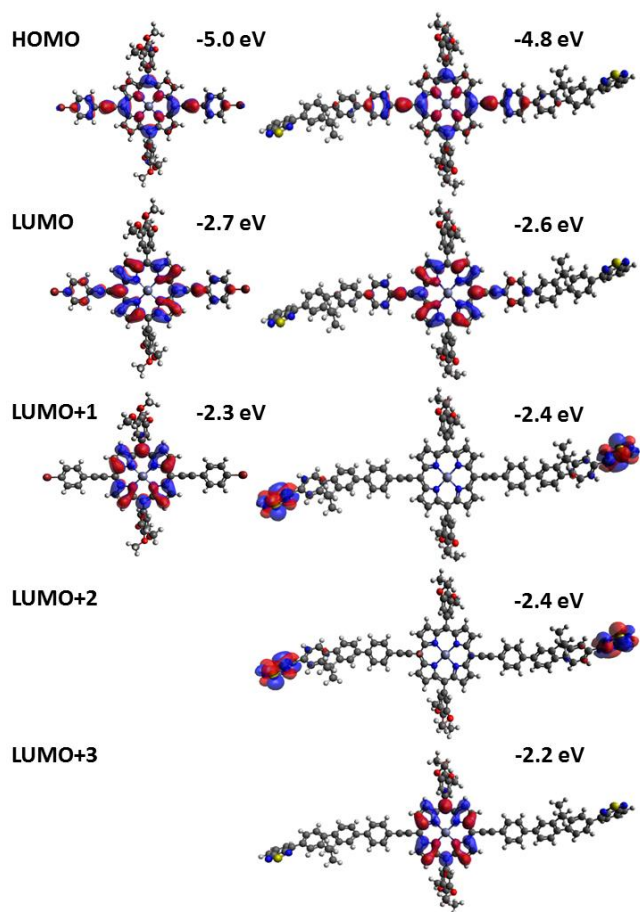


Figure 8. The molecular orbitals of a F8BT-HAPAPP model and HAPAPP calculated using B3LYP/6-31G(d). Note that the LUMO+1 and LUMO+2 of F8BT-HAPAPP are isoenergetic and identical except for an inversion of the wavefunction phase symmetry.

However, there is also some evidence of the F8BT triplet occurring during 518 nm excitation of F8BT-HAPAPP (**Figure 6c**). At early times, prior to approximately 50 μs , the F8BT-HAPAPP spectrum closely resembles that of the F8BT triplet on the red side of the 780 nm peak. The blue side shows distinct evidence of the negative porphyrin Q band bleach, which interferes with the positive triplet signal, distorting the band shape in this region. Nevertheless, the porphyrin bleach is substantially weaker in the case of 518 nm compared to 650 nm excitation at early times, suggesting the presence of a stronger positive signal (the F8BT triplet). At longer times, as mentioned above, the spectrum evolves to resemble the porphyrin. As such, the $\tau = 19$ μs component of the F8BT-HAPAPP decay is very likely triplet energy transfer from the F8BT to the porphyrin.

The μs -TAS experiments were repeated in the solid state. Film samples of F8BT-HAPAPP showed clear evidence of porphyrin triplet states, irrespective of excitation wavelength (**Figure S4**).

Discussion

The microsecond TA spectra clearly show that F8BT excitation of F8BT-HAPAPP results in the formation of a porphyrin triplet at long timescales. The formation of this triplet can take place in one of two ways: singlet energy transfer from F8BT to HAPAPP followed by ISC in the porphyrin units, or via direct triplet energy transfer from F8BT to HAPAPP. The results presented above suggest that both mechanisms are present simultaneously.

The singlet energy transfer mechanism (which alternatively could be considered internal conversion to a lower energy singlet state) is expected to be a much faster process than spin-forbidden ISC in F8BT and thus should dominate for those F8BT excitons formed near a porphyrin unit. The presence of this singlet energy transfer pathway is supported by the ps-TAS data, with the appearance of an additional fast decay component in the F8BT-HAPAPP singlet decay dynamics. Only those F8BT singlets generated close enough to a porphyrin unit will ultimately generate a porphyrin triplet via this pathway. Those F8BT singlets generated beyond the F8BT exciton diffusion length of ~ 8 nm³⁴ to a porphyrin unit will exhibit standard F8BT photophysics. It is estimated from the fitting that 80 % of F8BT excitons undergo the standard F8BT relaxation processes (primarily fluorescence but also, crucially, ISC), while approximately 20 % undergo energy transfer to the lower energy porphyrin singlet. This low transfer efficiency accounts for the smaller porphyrin triplet signal amplitude observed when exciting the F8BT component of F8BT-HAPAPP compared to porphyrin excitation (**Figure S5**). The lack of observation of the porphyrin triplet in the ps spectra upon 518 nm excitation of F8BT-HAPAPP is therefore a combination of the low efficiency of the energy transfer process and the intense, broad F8BT singlet band obscuring the weaker triplet bands. The presence of this additional singlet energy transfer pathway is consistent with the appreciable reduction in F8BT fluorescence quantum yield when the porphyrin is introduced into the polymer backbone. The timescale of singlet energy transfer (~ 140 ps) is shorter than that of F8BT fluorescence (~ 2 ns), and thus provides an effective competing relaxation pathway for F8BT singlet states generated close to a porphyrin, thereby reducing the F8BT fluorescence quantum yield.

For those F8BT singlet excitons that form further than ~ 8 nm from a porphyrin unit, standard F8BT relaxation pathways apply. A small percentage of the excitons will undergo intersystem crossing to the F8BT triplet ($\phi_{ISC} < 0.2$). It is known that the F8BT triplet exciton diffusion length of 180 nm²⁴ is much longer than that of the singlet, and thus it is likely that most F8BT triplets will be able to diffuse and encounter a porphyrin unit within their microsecond lifetime. This is consistent with the μ s-TAS results, which show a spectral evolution from F8BT to porphyrin triplets with 518 nm excitation. Furthermore, the presence of an additional 518 nm excitation decay phase that is both faster

than either of the pristine controls (19 μ s) and absent during direct porphyrin excitation is consistent with triplet energy transfer that occurs after microsecond timescale triplet exciton diffusion has taken place.

The proposed photophysical mechanism taking place during excitation of F8BT-HAPAPP is shown in **Figure 7** (the control molecules' mechanisms are displayed in **Figure S6**). It is therefore likely that the mechanism of porphyrin triplet formation in F8BT-HAPAPP occurs via a dual pathway mechanism. The faster process, dominating for F8BT excitons generated close to the porphyrins, is through an initial singlet energy transfer process from F8BT to HAPAPP, followed by ISC. The slower process, for F8BT singlet excitons generated within the bulk of the F8BT polymer, involves initial ISC to the longer lived F8BT triplet followed by diffusion to a porphyrin unit, where triplet energy transfer takes place.

The porphyrin triplet lifetime of F8BT-HAPAPP is less than half that of the pristine porphyrin, and substantially longer than the F8BT triplet. Such behaviour has been observed before in a different porphyrin hybrid polymer¹⁹ and was attributed to an energy transfer equilibrium between the porphyrin and polymer triplet populations. However, in that case no spectral evolution was observed. In contrast, the μ s-TAS of F8BT-HAPAPP shows a clear evolution from the F8BT triplet to the porphyrin triplet on the early microsecond timescale when exciting the F8BT. Furthermore, the F8BT-HAPAPP porphyrin triplet decay is mono-exponential and thus no higher order quenching effects from clustering of the porphyrins together in the polymer chain are evident.

DFT (B3LYP/6-31G(d)) calculations on a F8BT-HAPAPP model (**Figure 8**) combined with a Mulliken orbital composition analysis³⁵ show that the molecular orbital density of both HOMO and LUMO partially extend across the F8BT in addition to the porphyrin (6.5 and 7.2 % of the total orbital density, respectively, are located on the F8BT). This greater delocalisation of the hybrid system's frontier molecular orbitals is made possible by the additional alkyne bond enhancing the planarity of the porphyrin relative to the polymer chain. The previously published hybrid polymer¹⁹ has a much more twisted structure, reducing the possibility of delocalisation of the porphyrin MOs onto the polymer chain. Another relevant observation is that the F8BT-HAPAPP model has two isoenergetic benzothiadiazole-localised unoccupied MOs (LUMO+1/+2) that are interposed between the energetically close porphyrin-based LUMO and LUMO+3 (the latter is identical to the pristine porphyrin's LUMO+1). Given the closeness in energy of these benzothiadiazole- and porphyrin-localised unoccupied MOs, orbital mixing is expected. This hypothesis was investigated further via TD-DFT calculations (**Table S1**, Supporting Information). Although triplet energies are unlikely to be highly accurate using this method, the transi-

tion contributions to each excited state are the relevant parameter for this work. As expected, the T₁ state of the porphyrin is calculated to involve a simple HOMO-LUMO transition. TD-DFT calculations on the F8BT-HAPAPP, however, suggest multiple transitions contribute to the T₁ state. The expected porphyrin-based HOMO-LUMO dominates, but an appreciable contribution from the HOMO→LUMO+2 transition, which involves the F8BT's benzothiadiazole, is also present. It is known from the literature that the T₁ state of F8BT is localised on the benzothiadiazole.²⁹ As such, the T₁ state of F8BT-HAPAPP appears to have dual HAPAPP/F8BT character, creating a triplet lifetime intermediate between the two pristine materials.

Conclusions

In this work a zinc porphyrin / F8BT hybrid polymer, with an approximate proportion of porphyrin of 10 % by weight, was synthesised and a photophysical study performed. It was observed that the end result of photoexcitation was the porphyrin triplet, irrespective of whether the F8BT or porphyrin units were excited. Two triplet formation pathways are active upon F8BT excitation, depending upon the location of the initially generated F8BT exciton. Those excitons formed within the F8BT singlet diffusion length to a porphyrin underwent singlet energy transfer, followed by ISC to create the porphyrin triplet. The excitons formed within the bulk of the F8BT polymer displayed standard F8BT decay pathways, with the small proportion of F8BT triplets generated via ISC able to diffuse to the porphyrin units and undergo triplet energy transfer. The F8BT-HAPAPP triplets thus produced have a lifetime intermediate between the two control materials. This intermediate lifetime was assigned to orbital mixing of energetically close porphyrin- and benzothiadiazole-based unoccupied molecular orbitals, leading to a mixed F8BT/porphyrin triplet state.

ASSOCIATED CONTENT

Supporting Information available: Steady state absorption showing Q band matching concentrations, excitation density independent ps-TA decay kinetics and fittings, lack of spectral signal from F8BT when exciting at 650 nm, film μs-TA spectra, μs-TA kinetics of the different samples corrected for photons absorbed, photophysical mechanisms for F8BT and HAPAPP, and all synthetic details.

AUTHOR INFORMATION

Corresponding author

*tracey.clarke@ucl.ac.uk

ACKNOWLEDGMENT

We would like to thank Professor James Durrant for the use of his ps-TAS system at Imperial College London. TMC would like to acknowledge support from EPSRC project EP/N026411/1. HB would like to acknowledge ERC grant CONTREX 679789 - 455.

REFERENCES

- (1) Köhler, A.; Bässler, H. Triplet States in Organic Semiconductors. *Mater. Sci. Eng.* **2009**, *66*, 71-109.
- (2) Freeman, D. M. E.; Musser, A. J.; Frost, J. M.; Stern, H. L.; Forster, A. K.; Fallon, K. J.; Rapidis, A. G.; Cacialli, F.; McCulloch, I.; Clarke, T. M.; *et al.* Synthesis and Exciton Dynamics of Donor-Orthogonal Acceptor Conjugated Polymers: Reducing the Singlet-Triplet Energy Gap. *JACS* **2017**, *139*, 11073-11080.
- (3) Ogawa, T.; Yanai, N.; Monguzzi, A.; Kimizuka, N. Highly Efficient Photon Upconversion in Self-Assembled Light-Harvesting Molecular Systems. *Sci. Rep.* **2015**, *5*, 10882.
- (4) Simpson, C.; Clarke, T. M.; MacQueen, R. W.; Cheng, Y. Y.; Trevitt, A. J.; Mozer, A. J.; Wagner, P.; Schmidt, T. W.; Nattestad, A. An Intermediate Band Dye-Sensitised Solar Cell Using Triplet-Triplet Annihilation. *Phys. Chem. Chem. Phys.* **2015**, *17*, 24826-24830.
- (5) Smith, M. B.; Michl, J. Singlet Fission. *Chem. Rev.* **2010**, *110*, 6891-6936.
- (6) Davis, N. J. L. K.; Allardice, J. R.; Xiao, J.; Petty, A. J.; Greenham, N. C.; Anthony, J. E.; Rao, A. Singlet Fission and Triplet Transfer to Pbs Quantum Dots in Tips-Tetracene Carboxylic Acid Ligands. *J. Phys. Chem. Lett.* **2018**, *9*, 1454-1460.
- (7) Huang, T.; Jiang, W.; Duan, L. Recent Progress in Solution Processable Tadf Materials for Organic Light-Emitting Diodes. *J. Mater. Chem. C* **2018**, *6*, 5577-5596.
- (8) Etherington, M. K.; Gibson, J.; Higginbotham, H. F.; Penfold, T. J.; Monkman, A. P. Revealing the Spin-Vibronic Coupling Mechanism of Thermally Activated Delayed Fluorescence. *Nat. Commun.* **2016**, *7*, 13680.
- (9) Clarke, T.; Ballantyne, A.; Jamieson, F.; Brabec, C.; Nelson, J.; Durrant, J. Transient Absorption Spectroscopy of Charge Photogeneration Yields and Lifetimes in a Low Bandgap Polymer/Fullerene Film. *Chem. Commun.* **2009**, *1*, 89-91.
- (10) Eng, M. P.; Barnes, P. R. F.; Durrant, J. R. Concentration-Dependent Hole Mobility and Recombination Coefficient in Bulk Heterojunctions Determined from Transient Absorption Spectroscopy. *J. Phys. Chem. Lett.* **2010**, *1*, 3096-3100.
- (11) Guo, J.; Ohkita, H.; Bente, H.; Ito, S. Near-Ir Femtosecond Transient Absorption Spectroscopy of Ultrafast Polaron and Triplet Exciton Formation in Polythiophene Films with Different Regioregularities. *JACS* **2009**, *131*, 16869-16880.
- (12) Guo, J.; Ohkita, H.; Yokoya, S.; Bente, H.; Ito, S. Bimodal Polarons and Hole Transport in Poly(3-Hexylthiophene):Fullerene Blend Films. *JACS* **2010**, *132*, 9631-9637.
- (13) Ohkita, H.; Cook, S.; Astuti, Y.; Duffy, W.; Tierney, S.; Zhang, W.; Heeney, M.; McCulloch, I.; Nelson, J.; Bradley, D. D. C.; *et al.* Charge Carrier Formation in Polythiophene/Fullerene Blend Films Studied by Transient Absorption Spectroscopy *JACS* **2008**, *130*, 3030-3042.
- (14) Ruseckas, A.; Theander, M.; Andersson, M. R.; Svensson, M.; Prato, M.; Inganäs, O.; Sundstrom, V. Ultrafast Photogeneration of Inter-Chain Charge Pairs in Polythiophene Films. *Chem. Phys. Lett.* **2000**, *322*, 136-142.
- (15) Saeki, A.; Seki, S.; Koizumi, Y.; Tagawa, S. Dynamics of Photogenerated Charge Carrier and Morphology Dependence in Polythiophene Films Studied by in Situ Time-Resolved Microwave Conductivity and Transient Absorption Spectroscopy. *J. Photoch. Photobiol. A* **2007**, *186*, 158-165.
- (16) Shoaee, S.; Eng, M. P.; Espildora, E.; Delgado, J. L.; Campo, B.; Martin, N.; Vanderzande, D.; Durrant, J. R. Influence of Nanoscale Phase Separation on Geminate Versus Bimolecular Recombination in P3ht:Fullerene Blend Films. *Energ. Environ. Sci.* **2010**, *3*, 971-976.
- (17) Subramanian, S.; Xin, H.; Kim, F. S.; Shoaee, S.; Durrant, J. R.; Jenekhe, S. A. Effects of Side Chains on Thiazolothiazole-Based Copolymer Semiconductors for High Performance Solar Cells. *Adv. Energy Mat.* **2011**, *1*, 854-860.
- (18) Yamamoto, S.; Ohkita, H.; Bente, H.; Ito, S. Role of Interfacial Charge Transfer State in Charge Generation and

- Recombination in Low-Bandgap Polymer Solar Cell. *J. Phys. Chem. C* **2012**, *116*, 14804-14810.
- (19) Andernach, R.; Utzat, H.; Dimitrov, S. D.; McCulloch, I.; Heeney, M.; Durrant, J. R.; Bronstein, H. Synthesis and Exciton Dynamics of Triplet Sensitized Conjugated Polymers. *JACS* **2015**, *137*, 10383-10390.
- (20) Rogers, J. E.; Nguyen, K. A.; Hufnagle, D. C.; McLean, D. G.; Su, W.; Gossett, K. M.; Burke, A. R.; Vinogradov, S. A.; Pachter, R.; Fleitz, P. A. Observation and Interpretation of Annulated Porphyrins: Studies on the Photophysical Properties of Meso-Tetraphenylmetalloporphyrins. *J. Phys. Chem. A* **2003**, *107*, 11331-11339.
- (21) Harriman, A. Luminescence of Porphyrins and Metalloporphyrins. Part 3.-Heavy-Atom Effects. *J. Chem. Soc., Faraday Trans. 2* **1981**, *77*, 1281-1291.
- (22) Islangulov, R. R.; Lott, J.; Weder, C.; Castellano, F. N. Noncoherent Low-Power Upconversion in Solid Polymer Films. *JACS* **2007**, *129*, 12652-12653.
- (23) Singh-Rachford, T. N.; Lott, J.; Weder, C.; Castellano, F. N. Influence of Temperature on Low-Power Upconversion in Rubbery Polymer Blends. *JACS* **2009**, *131*, 12007-12014.
- (24) Wallikewitz, B. H.; Kabra, D.; Gélinas, S.; Friend, R. H. Triplet Dynamics in Fluorescent Polymer Light-Emitting Diodes. *Phys. Rev. B* **2012**, *85*, 045209.
- (25) Köhler, A.; Beljonne, D. The Singlet-Triplet Exchange Energy in Conjugated Polymers. *Adv. Func. Mater.* **2004**, *14*, 11-18.
- (26) Kuimova, M. K.; Hoffmann, M.; Winters, M. U.; Eng, M.; Balaz, M.; Clark, I. P.; Collins, H. A.; Tavender, S. M.; Wilson, C. J.; Albinsson, B.; *et al.* Determination of the Triplet State Energies of a Series of Conjugated Porphyrin Oligomers. *Photochem. Photobio. Sci.* **2007**, *6*, 675-682.
- (27) Walters, V. A.; de Paula, J. C.; Jackson, B.; Nutaitis, C.; Hall, K.; Lind, J.; Cardozo, K.; Chandran, K.; Raible, D.; Phillips, C. M. Electronic Structure of Triplet States of Zinc(II) Tetraphenylporphyrins. *J. Phys. Chem.* **1995**, *99*, 1166-1171.
- (28) Esipova, T. V.; Vinogradov, S. A. Synthesis of Phosphorescent Asymmetrically Π -Extended Porphyrins for Two-Photon Applications. *J. Org. Chem.* **2014**, *79*, 8812-8825.
- (29) Ford, T. A.; Avilov, I.; Beljonne, D.; Greenham, N. C. Enhanced Triplet Exciton Generation in Polyfluorene Blends. *Phys. Rev. B* **2005**, *71*, 125212.
- (30) Moravec, D. B.; Lovaasen, B. M.; Hopkins, M. D. Near-Infrared Transient-Absorption Spectroscopy of Zinc Tetraphenylporphyrin and Related Compounds. Observation of Bands That Selectively Probe the S_1 Excited State. *J. Photoch. Photobio. A* **2013**, *254*, 20-24.
- (31) Pekkarinen, L.; Linschitz, H. Studies on Metastable States of Porphyrins. II. Spectra and Decay Kinetics of Tetraphenylporphine, Zinc Tetraphenylporphine and Bacteriochlorophylli. *JACS* **1960**, *82*, 2407-2411.
- (32) Lee, C.-L.; Yang, X.; Greenham, N. C. Determination of the Triplet Excited-State Absorption Cross Section in a Polyfluorene by Energy Transfer from a Phosphorescent Metal Complex. *Phys. Rev. B* **2007**, *76*, 245201.
- (33) A.S., D.; N.C., G. Triplet Formation in Polyfluorene Devices. *Adv. Mater.* **2002**, *14*, 1834-1837.
- (34) Tamai, Y.; Ohkita, H.; Bente, H.; Ito, S. Exciton Diffusion in Conjugated Polymers: From Fundamental Understanding to Improvement in Photovoltaic Conversion Efficiency. *J. Phys. Chem. Lett.* **2015**, *6*, 3417-3428.
- (35) Lu, T.; Chen, F. Multiwfn: A Multifunctional Wavefunction Analyzer. *J. Comput. Chem.* **2012**, *33*, 580-592.

TOC graphic

